



Modeling the variability in phenology-based growth dynamics of *Spartina alterniflora* with latitude

Yejin Jung

Marine Research Division, Korea Maritime Institute, Busan, Republic of Korea



ABSTRACT

The variation in dynamics of translocation between above- and below-ground biomass of *Spartina alterniflora*, the dominant blue carbon source in North American saltmarshes, was studied across latitude using Phenology-based Growth dynamic model (PG model). The study shows that the main sources of the carbon translocation to the below-ground tissues varies with latitude. The model analysis suggests both photosynthates and the remobilization of assimilates during growing and senescing periods serve as the main sources of the carbon translocation from above-to below-ground tissues in a higher latitude. However, in the lower latitude regions with a warmer environment, the main source to build up the below-ground biomass was the immediate photosynthesis that occurred during growing seasons. The total photosynthates translocation from above-to below-ground tissues during growing seasons increase as the latitude decreases, whereas the assimilates translocation from the senescing shoots to below-ground during fall seasons increases as latitude increases. Assimilates are allocated from below-to above-ground tissues during the dormancy period in higher latitude. The model enables us to predict both above- and below-ground biomass and quantify the carbon translocation, which helps us understand the main sources of allocation to the below-ground tissues, a critical component of potential blue carbon sequestration, at different phenological events.

1. Introduction

Spartina alterniflora, a dominant saltmarsh species along the U.S. and European coastlines, serves as a critical climate regulator owing to its significant blue carbon sequestration capabilities (Davis et al., 2015; Unger et al., 2016). It is also increasingly identified as an invasive species, expanding into diverse coastal wetlands worldwide, including regions in Australia, South Africa, and East Asia (Ning et al., 2021; Qi and Chmura, 2023). Phenology, the study of life history event timings in plant and animal life, such as bud-burst, leaf-expansion, flowering, and abscission in plants, is influenced by seasonal and inter-annual climate variations, environmental, and habitat factors (Fenner, 1998). The phenology of *S. alterniflora* varies geographically; for instance, in Nova Scotia, Canada, green-up occurs in April with peak biomass in October (Cranford et al., 1989), while in South Carolina, the U.S., aerial growth starts in March, peaking in September (Morris and Haskin, 1990). Flowering times also differ in the U.S., beginning between September and November in Mississippi (Eleuterius and Caldwell, 1984) and in late July in South San Francisco Bay (Callaway and Josselyn, 1992). Although phenology is affected by abiotic factors such as temperature and precipitation on local scales (O'Donnell and Schalles, 2016), it is considered to be largely determined genetically. For example, Crosby et al. (2015) found from their greenhouse mesocosm experiment in the U.S. that northern marsh *S. alterniflora* from Massachusetts and

Delaware flowered earlier (July–August) than plants from more southern marshes from North and South Carolina regions (October).

Phenology has been shown to be an effective indicator of the success of competition in community and growth dynamics of both above and below-ground biomass. In San Francisco bay, *S. alterniflora* begin spring growth approximately one month earlier than *Spartina foliosa* and are taller than *S. folis* with differences being greater than 60 cm (Callaway, 1990) and thus contain more live above-ground biomass throughout the year (Callaway and Josselyn, 1992). Crosby et al. (2015) found that the onset of flower production leads to an increase in the below-ground allocation. Moreover, below-ground biomass and non-structural carbohydrate (NSC) content in *S. alterniflora* increase with latitude, as evidenced by higher below-ground production in Delaware compared to South Carolina and varying NSC levels in Nova Scotia and Georgia (Dame and Kenny, 1986; Roman and Daiber, 1984; Livingstone and Patriquin, 1981; Jung and Burd, 2017). This pattern suggests that earlier flowering in northern regions prompts earlier biomass allocation to below-ground tissues, aiding winter survival and subsequent seasonal growth (Lytle and Hull, 1980). However, the details of carbon translocation across various phenological stages are not yet fully understood.

Understanding plant phenology and translocation dynamics is essential for quantifying growth and carbon allocation. Phenology-based models have been utilized to study local to latitudinal phenology shifts (Kramer, 1994; Chuine et al., 2000; Cleland et al.,

E-mail address: yjjung@kmi.re.kr.

Table 1

Characteristic of three regions (Delaware, South Carolina, and Louisiana) in latitudinal study using the PG model.

Delaware (DE) (lat: 38.79, long: 75.16)		South Carolina (SC) (lat: 33.32, long: 79.17)	Louisiana (LA) (lat: 29.25, long: 90.66)
Data reference	Roman and Daiber (1984)	Dame and Kenny (1986)	Darby and Turner (2008)
Study site	The Blackbird Creek marsh, DE	The high marsh site covered by short Spartina and located at the upper reaches of Bly Creek side in North inlet, SC	Salt marsh located 0.5 km west of the Louisiana University Marine Consortium laboratory, in Cocodrie, LA
Form of <i>S. alterniflora</i>	Tall form <i>S. alterniflora</i>	Tall form <i>S. alterniflora</i>	Inland form <i>S. alterniflora</i> ^a
Periods of field data	monthly data for both above- and below-ground data from Feb. 1975 to Oct. 1976	monthly data for above-ground data and bimonthly data for below-ground data from Jun. 1983 to May 1984	monthly data for both above- and below-ground data from Mar. 2004 to Mar. 2005
Salinity ranges	25~30 ppt (The average value, 27.5 ppt was applied in the model)	17~36 ppt (The average value, 30.01 ppt was applied in the model)	7~20 ppt (The average value, 13.5 ppt was applied in the model)

^a Inland form *S. alterniflora* in the microtidal environment such as the study site in Louisiana indicates the *S. alterniflora* that has a height ranging from 0.8 m to 1.2 m and grows 2 m from the water's edge and represent 80~90 % of the total salt marsh landscape (Turner and Gosselink, 1975; Darby and Turner, 2008).

2007), forecast species range (Bertin, 2008; Chuine and Beaubien, 2001; Ehrlén and Morris, 2015) and productivity shifts (Euskirchen et al., 2014; Heimann et al., 1998; Van Wijk and Williams, 2003), and analyze plant responses to abiotic changes. Zheng et al. (2016) developed a model for *S. alterniflora*, integrating phenological stages and bidirectional material translocation, building upon models for *Typha* species and *Phragmites australis* (Asaeda and Karunaratne, 2000; Asaeda et al., 2005). This model, covering a wide geographic range, highlights regional root-to-shoot ratio differences but requires additional data for implementation, such as aged one year and older rhizomes' mortality and respiration rates.

In this study, we applied the Phenology-based Growth (PG) model (Jung and Burd, 2024), combining aspects of Morris et al.'s production model (1984) and the Zheng et al. model (2016), with added effects of salinity on plant production. The model serves a dual purpose: as an inverse model, it aids in ascertaining the values of undisclosed parameters that align best with the observed biomass; and as a forward model, it forecasts biomass, translocation, and daily production over the course of a year. In our model, the dormancy phase is defined as the time span in which the below-ground plant structures remobilize assimilates and translocate their soluble carbon to the above-ground biomass. This phase supports above-ground survival through winter, facilitates early spring growth, and coincides with a period of inactivity in plant growth despite the availability of adequate irradiance for photosynthesis. We

employ the PG model to analyze how translocation between biomass compartments varies with latitude and environmental factors, influencing life-history event timings. By applying site-specific data, this theoretical study elucidates phenological variability and its impact on below-ground allocation across different latitudes, offering new insights into carbon transfers in blue carbon ecosystems.

Our research questions are (1) Does the model predict differences in the importance of winter below-ground storage between *S. alterniflora* growing in colder vs. warmer climates? (2) How do the rates and amounts of translocated material during growth, senescence, and dormancy periods differ for *S. alterniflora* by latitude? (3) How do seasonal mortality and respiration rates of *S. alterniflora* change with latitude? We hypothesize that, (1) *S. alterniflora* at lower latitudes translocates more biomass from above-to below-ground tissues during the growing period compared to *S. alterniflora* in higher latitudes. (2) The carbon translocation from senescing shoots increases as the latitude increases.

2. Methods and materials

2.1. Study sites

We chose data from locations at three different latitudes, Delaware (38.79° N, -75.16° W), South Carolina (33.32° N, -79.17° W), and Louisiana (29.25° N, -90.66° W) in the U.S. Firstly, our site selection criterion mandated the use of the Smalley harvesting method (Smalley, 1958), acknowledging its comprehensive approach in accounting for changes in both live and dead above-ground biomass. This method is chosen due to its demonstrated superiority in providing more accurate production estimates compared to the peak live standing crop method, especially given the significant disparities in production estimates arising from different methodologies (Roman and Daiber, 1984). Secondly, we specifically included studies that reported biomass measurements for *S. alterniflora* with heights exceeding 0.8 m in saline wetlands. This selection was aimed at investigating the near-tall form of *S. alterniflora* (Table 1).

2.2. Biotic variables

At each of the three locations, the ratio of live above-ground biomass to total above-ground biomass was used as an estimate of the green-leaf ratio required by the model. The sum of live and dead biomass was used for the observed above-ground biomass and only live below-ground biomass was used for the observed below-ground biomass. The sum of live and dead below-ground biomass was available in Delaware site (Roman and Daiber, 1984), so we calculated the live below-ground biomass using the tall *S. alterniflora* live:dead below-ground biomass ratio measured in Delaware by Gross et al. (1991). Leaf nitrogen data was either available as a yearly average value (Roman and Daiber, 1984) or less than 4% (Darby and Turner, 2008). Morris (1982) demonstrated

Table 2
Definitions of symbols and parameter values.

Symbol	Name	Units & Value
E_0	Ratio of Sun-Earth distance to mean distance	Dimensionless
A_f	Solar constant	1367 W m ⁻²
S_c	Atmospheric absorption	0.4 Dimensionless
Z	Zenith angle	Degree
P	Total net production	gdwt m ⁻² h ⁻¹
B_{above}	Above ground biomass	gdwt m ⁻²
B_{below}	Below ground biomass	gdwt m ⁻²
T	Air temperature	°C
θ	Solar elevation	Radians
L	Solar irradiance at the top of the canopy	W m ⁻²
λ	Half saturation constant for irradiance	300 ± 100 W m ⁻²
α	Irradiance extinction rate within the canopy	(3.4 ± 1.0) × 10 ⁻⁴ m ²
N	Percent of nitrogen in the dry leaves	gdwt ⁻¹
F	Ratio of green tissue to total canopy biomass	%
ψ	Temperature coefficient for gross production	(7.1 ± 1.7) × 10 ⁻⁴ °C ⁻¹
η	Half saturation constant for nitrogen	h ⁻¹
F	Green leave ratio	0.36 ± 0.29 % dwt
m_a	Specific rate of above-ground mortality at 20 °C	Percentage
m_b	Specific rate of below-ground mortality at 20 °C	gg ⁻¹ d ⁻¹
θ	Temperature constant	1.09

that the growth rate of *S. alterniflora* was found to be insensitive to the leaf-nitrogen concentrations between 1% and 4%. Therefore, we used a similar time series of nitrogen data for the independent variable in the production function for all simulations.

2.3. Abiotic variables

The calculated temperature and irradiance data at each latitude were used as the main input data in the model. The hourly temperature normal data from 1981 to 2010 at three different latitudes were acquired from U.S. climate normal products database from NOAA national centers for environmental information website (<https://www.ncdc.noaa.gov/data-access/land-based-station-data/land-based-datasets/climate-normals/1981-2010-normals-data>). The temperature normal is calculated by taking the average of the 30 hourly values from year 1981–2010 at each hour. These climatological temperatures were utilized to determine parameter values of the temperature equation (1) in Morris et al.'s model (1984) by using the temperature model described below in inverse mode. The temperature was modeled as

$$T = a_1 \sin(0.017D + a_2) + a_3 \sin(0.26H + 4.45) + a_4 \quad (1)$$

where T is temperature ($^{\circ}\text{C}$), D is the calendar day (1–365) and H is the hour (1–24).

The coefficient value, a_1 , describes the degree of seasonal amplitude in temperature wave. For example, if a_1 increases, the seasonal amplitude increases which in turn affects the annual maximum and minimum temperatures. The coefficient a_2 represents a phase shift of the seasonal temperature period. The positive and negative phase shift a_2 indicate a shift to the later or earlier, respectively. The coefficient value, a_3 , determines the amplitude of daily temperature. As a_3 increases, it gives the higher daily maximum temperature and the lower daily minimum temperature. Finally, the coefficient value, a_4 , represents a yearly offset. The positive and negative offset a_4 indicates a shift upward or downward, respectively. Values of the coefficients a_i enable us to quantify the amplitude and phase of seasonal and daily temperature variability at each latitude. The coefficients a_i were estimated by fitting equation (1) to the climatological temperatures using the cost function

$$Dt_i = \sum_i^n (NT_i - MT_i)^2 \quad (2)$$

where NT_i is climatological temperatures and MT_i is the modeled temperature at the i -th time point. The estimated parameters (Supple-

$$\text{dB}_{\text{above}} / \text{dt} = G - R_{\text{above}} - M_{\text{above}} - TB_{\text{above_to_below}} + TB_{\text{below_to_above}} - TP_{\text{above_to_below}} \quad (7)$$

mentary Table 1) were used to generate temperature data in the PG model for each latitude.

Irradiance (mW cm^{-2}) for each location was calculated using standard formulae (e.g. Iqbal, 1984). First, the ratio of Sun-Earth distance to mean Sun-Earth distance, E_0 was estimated using the following equation.

$$E_0 = 1.000110 + 0.034221 \cos(\Psi_e) + 0.001280 \sin(\Psi_e) + 0.000719 \cos(2\Psi_e) + 0.00077 \sin(2\Psi_e) \quad (3)$$

where,

$$\Psi_e = \left(\frac{2\pi}{365} \right) (D-1) \quad (4)$$

Finally, the irradiance (L) was estimated by the following equation.

$$L = \left(A_f S_c E_0 \cos \left(\frac{Z\pi}{180} \right) \right) \quad (5)$$

where A_f is a solar constant and S_c is an atmospheric absorption coefficient (Table 2). Z is the zenith angle (in degrees) calculated using standard equations (Kirk, 1994). The hourly irradiance was calculated only for times between sunrise and sunset.

2.4. Model formulation

2.4.1. Net primary production

The basic structure of the PG model (Jung and Burd, 2024) is shown schematically in Fig. 1.

For a clearer understanding of this study, the formulation of the PG model as developed by Jung and Burd (2024) is revisited and elaborated upon as follows. Gross production (G) and respiration rates were estimated using the model described in Morris et al. (1984). Gross production is a function of total canopy biomass, irradiance at the top of the canopy, solar elevation, air temperature, green-leaf ratio, and leaf nitrogen content (Equation (6)). Above- and below-ground respiration rates were calculated as functions of temperature, green-leaf ratio and biomass (Equation (6)). Total net production was then given by

$$P = \frac{\psi TNF \sin(\theta) \left\{ \ln \left(Le^{\frac{\alpha B_c}{\sin(\theta)}} + \lambda \right) - \ln(L + \lambda) \right\}}{(\alpha(N + \eta))} - \rho T (FB_{\text{above}} + B_{\text{below}}) \quad (6)$$

← Gross production → ← Respiration →

where the symbols and values for constants are given in Table 2.

Equation (6) does not include any explicit representation of translocation between above- and below-ground tissue, or mortality. To incorporate these flows, we included formulations for mortality and translocation between above- and below-ground tissues from the model developed by Zheng et al. (2016). Equations for the rates of above- and below-ground biomass were then written as a balance between production, respiration, mortality losses, and translocation

$$\text{dB}_{\text{below}} / \text{dt} = TB_{\text{above_to_below}} + TP_{\text{above_to_below}} - TB_{\text{below_to_above}} - R_{\text{below}} - M_{\text{below}} \quad (8)$$

where B , G , and R represent biomass, gross production rate, and respiration rate, while M , TB , and TP denote mortality rates, carbon translocation rates between above- and below-ground biomass and

photosynthate translocation rates between above- and below-ground biomass.

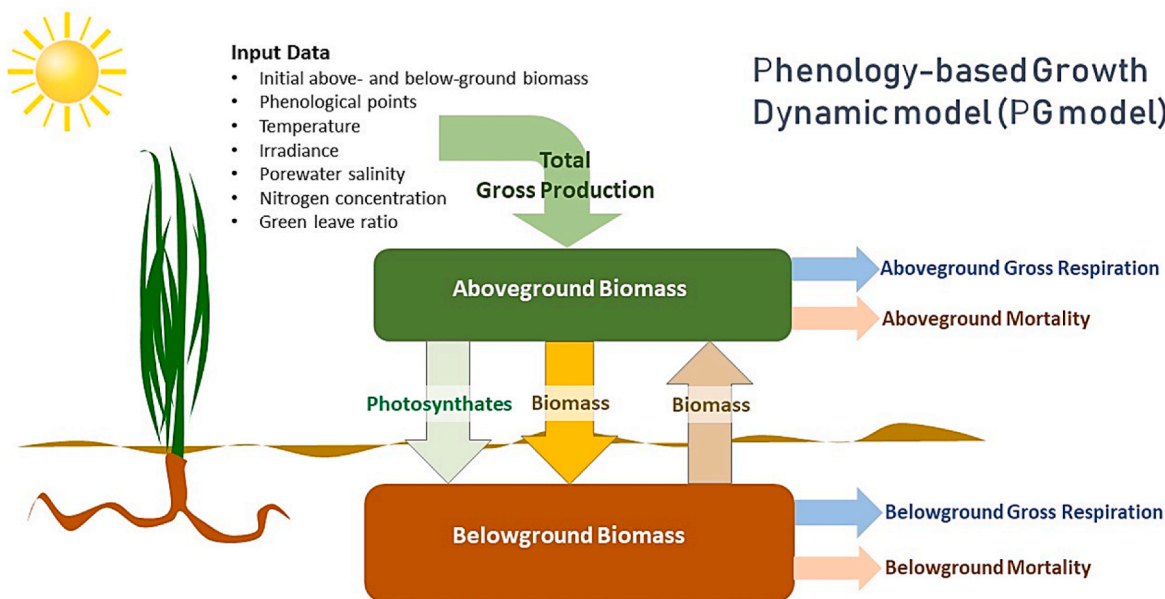


Fig. 1. Structure of the *S. alterniflora* Phenology-based Growth dynamic model (PG model) from (Jung and Burd, 2024)

The hourly mortality rate was described as a function of temperature and biomass (Zheng et al., 2016)

$$M_{\text{above}} = m_a \theta^{(T-20)} B_{\text{above}} \quad (9)$$

$$M_{\text{below}} = m_b \theta^{(T-20)} B_{\text{below}} \quad (10)$$

The parameter values of m_a and m_b for *S. alterniflora* at three different latitudes were estimated using the PG model in inverse mode (see below).

2.4.2. Carbon translocation and phenological dates

The carbon translocation rates between above- and below-ground tissues were calculated using the following equations (Zheng et al., 2016):

$$TP_{\text{above_to_below}} = \alpha_{ab} G \quad (11)$$

$$TB_{\text{above_to_below}} = \gamma B_{\text{above}} \quad (12)$$

$$TB_{\text{below_to_above}} = \alpha_{ba} \theta^{(T-20)} B_{\text{below}} \quad (13)$$

where $TP_{\text{above_to_below}}$ is the translocation rate of photosynthate from above-to below-ground tissues during the growing season, $TB_{\text{above_to_below}}$ is the assimilate translocation rate from above-to below-ground tissues during plant senescence, and $TB_{\text{below_to_above}}$ is the assimilate translocation rate from below-to above-ground tissues during the dormancy period. The definitions of symbols of parameters in Equations (11)–(13) are given in Table 3 and the local phenological dates of three locations in the PG model are shown in Table 4.

All dates are represented as numerical day-of-year with January 1st

Table 3
Definitions of symbols of parameters estimated in the inverse model.

Symbol	Name
α_{ab}	Fraction per hour of photosynthate translocated from above- to below-ground during growing period
α_{ba}	Fraction per hour of below-ground assimilate translocated from below- to above-ground during dormancy period
γ	Fraction per hour of above-ground assimilate translocated from above- to below-ground during senescence
m_a	Specific rate of above-ground mortality at 20 °C
m_b	Specific rate of below-ground mortality at 20 °C

Table 4

Site-specific phenological input data applied on the latitudinal study in the PG model.

	Delaware	South Carolina	Louisiana
SB _{below_to_above}	305 (Nov. 1)	349 (Dec. 15)	365 (Dec. 31)
EB _{below_to_above}	60 (Mar. 1)	46 (Feb. 15)	31 (Jan. 1)
SP _{above_to_below}	60 (Mar. 1)	46 (Feb. 15)	31 (Jan. 1)
EP _{above_to_below}	274 (Oct. 1)	288 (Oct. 15)	334 (Nov. 30)

being day 1. The major phenological dates (Table 4) and the corresponding phenological events in the present model are summarized as follows:

- 1) SB_{below_to_above}: the start date of the translocation of remobilization of below-ground assimilates to above-ground tissues during the dormancy period;
- 2) EB_{below_to_above}: the end date when below-ground remobilized assimilate is translocated to above-ground tissues during the dormancy period;
- 3) SP_{above_to_below}: the start date when the photosynthates from the above-ground tissues is translocated to below-ground tissues during the growing season;
- 4) EP_{above_to_below}: the end date for translocation of photosynthates from the above-ground tissues to below-ground tissues during the growing period, and the start date for the remobilization and translocation of assimilate from the above-ground senescing tissues to the below-ground tissues during the senescence period.

The phenological dates for *S. alterniflora* were estimated based on the timing of the first observation of senescing tissues in collected above-ground biomass, and by observing the seasonal above- and below-ground biomass patterns. To do this, the average monthly above- and below-ground biomass and their standard deviations were calculated at the three latitudes. A cubic spline was used to interpolate between the data points. When we observed a continuous decrease in below-ground biomass, we defined this period as the dormancy period. Once the dormancy period ends, environmental conditions become favorable for active growth, and the plants start to increase above-ground biomass. We denote this phenological point as SP_{above_to_below}, and the period between SP_{above_to_below} to the start of senescence (EP_{above_to_below}) as the growing period.

2.4.3. Effect of porewater salinity on the production of *S. alterniflora*

To account for the effects of salinity on production, we developed a salinity dependent factor that multiplied gross production. Equation (6) and its associated parameter values were derived from the *S. alterniflora* cultures under different shading and nitrogen levels (Morris, 1982); the average salinity of the water in these cultures was approximately 17.5 ppt. To incorporate the effects of variable salinity on production, we developed a parameterization of the effects of salinity on the gross production rate for *S. alterniflora* (Supplementary Fig. 1) based on data from studies of the relationship between salinity and production (Linthurst and Seneca, 1981; Ge et al., 2014).

This relationship provided a factor that multiplied the gross production and was designed such that it has a value of 1 for a salinity of 17.5 ppt environment. In developing this parameterization, we assumed that gross production was zero at salinities of 60 ppt and above based on reference data (Bertness and Ewanchuk, 2002).

Howes et al. (1981) reported that creek bank sediments have porewater salinity that is similar to that in the creek during the flooding tide because of frequent drainage. For the latitudinal study, it was assumed that the average porewater salinity at each site was the same as the water column salinity reported at the study site since *S. alterniflora* collected at the three sites were located within 20 m of the creek bank. The average porewater salinities for study sites in Delaware, South Carolina, and Louisiana were set as 27.5 ppt, 30.01 ppt, and 13.5 ppt by selecting the mid-point of the stated salinity range at the site (Roman and Daiber, 1984; Darby and Turner, 2008) or by calculating the average salinity when seasonal salinity values were available (Dame and Kenny, 1986).

2.4.4. The inverse model

To determine the values of the parameters used in the PG model (Table 3), we used the model in inverse mode allowing us to find the values of the parameters that best fit the observed biomasses between October 2013 and December 2014. To do this, we minimized the cost function

$$\chi^2 = \sum_{i=t_s}^{t_e} \frac{((\text{observed } AG_i - \text{modeled } AG_i)^2 + (\text{observed } BG_i - \text{modeled } BG_i)^2)}{\sigma_i^2} \quad (14)$$

where, t_s is the date of the first observation, t_e is the time of the last observation, *observed AG* and *observed BG* are the field above- and below-ground biomass at i -th time point. The *observed AG* biomass was obtained through the allometry equation which calculates the above-ground biomass using the relationship of plant height. The plant heights of all shoots taller than 10 cm were measured at the center of each plot within the quadrat. The *observed BG* is acquired by multiplying the root: shoot ratio obtained from the monthly destructive core samples to the *observed AG* biomass. *Modeled AG* and *modeled BG* are the calculated above- and below-ground biomass in the PG model at i -th time point. The cost function was minimized using a constrained nonlinear minimization routine (the Matlab function fmincon) employing an interior point algorithm. The *S. alterniflora* model was used in inverse mode for each of three locations of *S. alterniflora* individually.

2.4.5. Forward model and numerical methods

The forward model simulations were run by solving equations (7) and (8) using the translocation and mortality parameter values for salinity ranges corresponding to three regions where *S. alterniflora* were found. Equations (7) and (8) for above- and below-ground biomass we solved using a 4th order Runge-Kutta method (e.g. Press et al., 2002) with a constant time step of 1 h. All computer codes were written and run using Matlab 2016b. Forward simulations were run and the model results were compared with corresponding observed above- and below-ground biomass.

The differences between observed and modeled biomass, ΔD_i , were

quantified based on the following equations

$$\Delta D_{a_i} = \frac{(\text{observed } AG_i - \text{modeled } AG_i)}{\sigma_i} \quad (15)$$

$$\Delta D_{b_i} = \frac{(\text{observed } BG_i - \text{modeled } BG_i)}{\sigma_i} \quad (16)$$

where, ΔD_{a_i} and ΔD_{b_i} are the differences in above-ground biomass and below-ground biomass normalized to the standard deviation of the field estimates.

3. Results

3.1. Parameter values from inverse model

The temperature inverse model estimated the coefficient values, a_i , for equation (1). Values of a_1 were highest in Delaware indicating that the differences between the annual minimum and maximum temperatures was greater there than that in Louisiana or South Carolina. The a_3 values, which indicate the extent of daily temperature fluctuations, were similar for all three latitudes (Supplementary Table 1).

The PG model was used in inverse mode to calculate the model parameters that gave the best fit of modeled biomass to observed biomass for *S. alterniflora* taller than 0.8 m in Delaware (DE), South Carolina (SC), and Louisiana (LA). The fraction of photosynthate translocated from above-to below-ground (α_{ab}) during the growing season was roughly similar ranging between 0.55 and 0.75 in all sites but the absolute amount of photosynthates translocation increases moving from higher to lower latitudes. The values of α_{ab} (Table 5) indicate that *S. alterniflora* at the three latitudes translocates more than half of its production generated from photosynthesis to the below-ground tissues during the growing season. In contrast, the fraction (γ) of above-ground assimilates translocated to below-ground tissues during the senescence period was highest in Delaware (0.0024) whilst plants in South Carolina and Louisiana had a lower and similar value (0.0006). This suggests that plants at higher latitudes rely on the carbon translocation from above-ground senescing tissues to a greater extent than plants at lower latitudes (SC and LA) for building up the below-ground biomass during the senescence period.

The fraction of below-ground assimilates translocated from below-to above-ground tissues (α_{ba}) during the dormancy period was highest in Delaware (1.3×10^{-5}) compared to that in South Carolina (4.7×10^{-13}) and Louisiana (1.2×10^{-14}). The fraction, α_{ba} , in Delaware seems reasonable value compared to the estimated value (8.2×10^{-4}) in Zheng et al.'s model (2016).

These model results indicate that *S. alterniflora* at higher latitudes translocates photosynthate to below-ground tissues during the growing season and assimilates from below-ground to above-ground tissues during the dormancy period. However, there is an apparent latitudinal difference in the relative amount of translocated material to the below-ground from different sources. The main source of carbon allocation to below-ground tissues at higher latitudes (DE) is a combination of photosynthate and senescing biomass, whereas it is mainly

Table 5

Parameter values from the inverse model run for the whole study period at each latitude and the sum of absolute values of ΔD_{a_i} and ΔD_{b_i} (Total ΔD_i) showing the level of differences between observed biomass and modeled biomass.

	<i>S. alterniflora</i> in DE	<i>S. alterniflora</i> in SC	<i>S. alterniflora</i> in LA
α_{ab} (fraction)	0.56	0.75	0.55
α_{ba} (fraction)	1.3×10^{-5}	4.7×10^{-13}	1.2×10^{-14}
γ (fraction)	0.0024	0.0006	0.0006
m_a ($\text{gg}^{-1} \text{d}^{-1}$)	0.0008	0.0006	0.0006
m_b ($\text{gg}^{-1} \text{d}^{-1}$)	0.0008	0.0006	0.0006
ρ ($^{\circ}\text{C}^{-1} \text{h}^{-1}$)	3.0×10^{-5}	1.5×10^{-5}	5.4×10^{-5}
Total ΔD_i	96.60	9.13	79.04

photosynthate in lower latitudes (LA).

The specific rate of both above- and below-ground mortality at 20 °C were very similar in all latitudes, ranging from 0.0006 to 0.0008 $\text{gg}^{-1} \text{d}^{-1}$.

The coefficient value for dark respiration, ρ , that was additionally included in the model for the latitudinal study, showed different values throughout all regions (Table 5). The ρ value was highest in Louisiana (5.4×10^{-5}) which is about two times than *S. alterniflora* in Delaware and four time higher than one in South Carolina. This ρ value in Louisiana was higher than the one on Sapelo Island, Georgia (2.3×10^{-5}). This is not surprising given the fact that the dark respiration rate increases with temperature and the highest air temperature were found in Louisiana.

The ΔD_i values, which quantify the differences between modeled and observed biomass, were lowest (9.13) in South Carolina which indicates that the model prediction showed good match with field data compared to Delaware (96.60), Louisiana (79.04) and the three height forms of *S. alterniflora* on Sapelo Island in Georgia ranging 57.64–77.07 (Table 5). Overall, the model accurately represented below-ground biomass in all three regions. However, larger deviations were noted in above-ground biomass in Delaware for most months, and in November in Louisiana, as shown in Fig. 2.

3.2. Above- and below-ground biomass derived from the PG model

During the early spring season (Jan., Feb.) the observed below-ground biomass in Delaware was more than four times greater than the above-ground biomass and then decreased continuously until July (Fig. 2a). The observed above-ground biomass, which included both dead and live biomass, remained less than 1500 g m^{-2} , and showed monthly variation throughout the late spring and fall but the annual variation was within 545 g m^{-2} . This relatively small variation compared to the one in below-ground was due to that the degree of the decreasing live above-ground biomass is similar to the increasing dead above-ground biomass throughout the year, so the sum of live and dead biomass stays consistent although the amount of the live above-ground

tissues that can actively photosynthesize fluctuates seasonally. The model reproduced the general behavior of the below-ground biomass but predicted larger than observed above-ground biomass in Delaware (Fig. 2a). Despite expectations for the inverse model in this latitudinal study to closely match observed data, notable deviations were observed in Delaware's above-ground biomass measurements throughout the year.

The model fit showed best agreement with the both above- and below-ground biomass in South Carolina (Fig. 2b). The modeled below-ground biomass in South Carolina ranged between approximately 1800–3000 g m^{-2} , which was about half of that seen in Delaware ranging from 2000 to 5000 g m^{-2} throughout the year (Fig. 2a & b). The modeled below-ground biomass in South Carolina stayed above 2500 g m^{-2} between September and January and then dropped to below 2000 g m^{-2} in May. The highest modeled above-ground biomass was observed in October in South Carolina, which agrees with the observed biomass (Fig. 2b).

Modeled Louisiana above-ground biomass successfully predicted the two peaks in fall (Sep.–Oct.) and in February. However, the model was not able to predict a winter minimum of above-ground biomass in November but instead predicted a minimum value in January. Overall, the modeled biomass indicated that Louisiana had the lowest average root:shoot ratio (0.92), compared to Delaware (2.51) and South Carolina (1.88).

3.3. Gross production and net production

The modeled gross production was almost 0 from January to May in Delaware but increased rapidly from May onwards and reached over 55 $\text{g m}^{-2} \text{d}^{-1}$ in September before decreasing in the following months (Fig. 3a).

The total plant net production was always less than 0 in Delaware indicating that *S. alterniflora* consumed more carbon through respiration of both above- and below-ground tissues than the carbon produced from photosynthesis during the study period. The negative net production, which corresponded with a decline in below-ground biomass, was

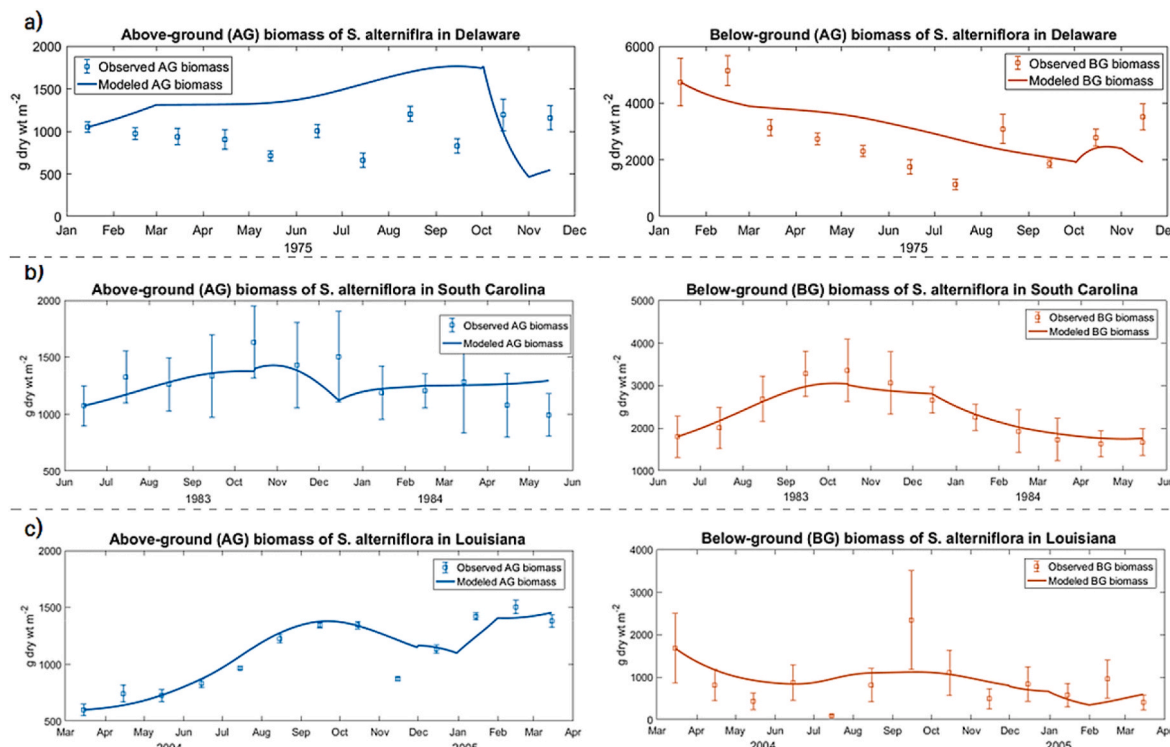


Fig. 2. Observed and modeled above- and below-ground biomass of *S. alterniflora* in Delaware(a), South Carolina(b), and Louisiana(c).

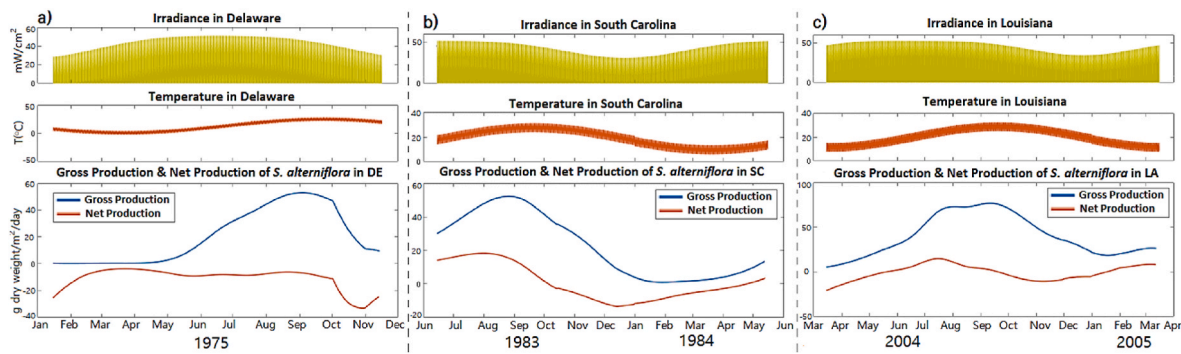


Fig. 3. Calculated irradiance, temperature, the estimated gross production and net production of the whole plant of *S. alterniflora* in Delaware(a), South Carolina(b), and Louisiana(c) in the PG model.

Table 6

Total carbon translocation at each phenological cycle at the three latitudes.

	Delaware	South Carolina	Louisiana
Total translocated photosynthate from above to below during growing season (g m^{-2})	2940	4363	7202
Total translocated biomass from above to below during senescence (g m^{-2})	1703	1252	458
Total translocated biomass from below to above during dormancy (g m^{-2})	261	2.6×10^{-6}	6.1×10^{-9}

observed (Fig. 2a), though a reduction in above-ground biomass was also noted.

Both gross production and net production in South Carolina were highest in late August and lowest between December and January (Fig. 3b), whereas the gross production in Louisiana was highest from July through early October (Fig. 3c).

Overall, the average daily gross production increased with decreasing latitude, and the patterns of gross production corresponded closely with the climatological temperature cycle at all sites (Fig. 3).

3.4. Translocated biomass at different phenological events

The amount of photosynthate or assimilate translocated during three periods at the three sites were estimated from the model. The largest amount (1703 g m^{-2}) of material translocated from above-to below-ground tissue during senescence occurred in tall *S. alterniflora* at the northern site (Delaware). This was approximately three times greater than the assimilate translocated during senescence at the Louisiana site (458 g m^{-2}) (Table 6).

A similar trend occurred for the assimilate translocated from below-ground to above-ground tissues during the dormancy period, where the assimilate translocation occurred at the Delaware site (261 g m^{-2}), whereas it was close to zero at South Carolina and Louisiana sites. Plants at the Louisiana site translocated the largest amount (7202 g m^{-2}) of photosynthate from above-to below-ground tissues during the growing

season, approximately 2.5 times greater than the amount translocated at the Delaware site (Table 6).

This pattern suggests that at higher latitudes below-ground biomass is sustained by the remobilization of assimilate from the senescing above-ground tissues. The photosynthate translocated from above-ground to below-ground through photosynthesis increased as latitude decreased, which supports our first hypothesis. This suggests that the below-ground biomass in lower latitudes is supported mainly by photosynthate translocated from above-ground during the growing season. The total assimilates allocated from below-to above-ground tissues during the dormancy period were highest in Delaware, compared to the almost zero value in South Carolina and Louisiana.

3.5. Mortality rates of above- and below-ground tissues

The mortality rates in both above- and below-ground tissues peaked in September to October in all three latitudes (Fig. 4). The highest and lowest mortality rates of below-ground tissues were observed in South Carolina and Louisiana, respectively. Overall, the mortality rates of below-ground biomass were more than two times greater than the above-ground mortality throughout the study periods except for the Louisiana site.

3.6. Respiration rates of above- and below-ground tissues

The respiration rates were high during October and low during spring at all three sites (Fig. 5). The daily mean above-ground respiration rate is highest in Louisiana, but its below-ground rate was similar at all three sites ranging from 17 to $24 \text{ g m}^{-2} \text{ d}^{-1}$ (Supplementary Table 2).

4. Discussion

Our first hypothesis that *S. alterniflora* growing in lower latitudes would translocate more biomass from above-to below-ground tissues, especially during the growing season, was supported by the study results. Our results showed that tall *S. alterniflora* growing at a lower latitude in a warmer environment translocate a greater proportion of its photosynthate to the below-ground biomass during the growing season

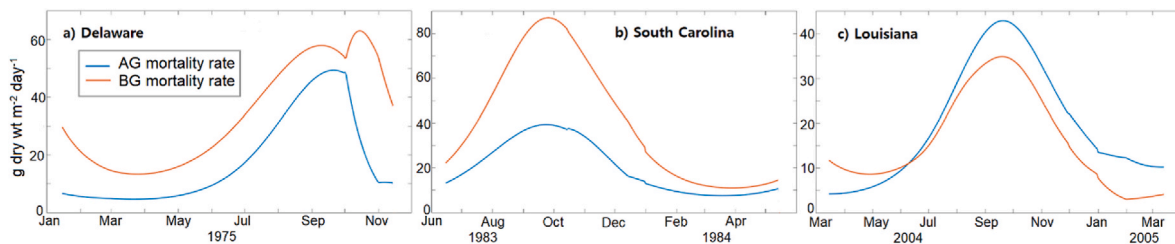


Fig. 4. Mortality rates of above- and below-ground biomass calculated in the PG model in the latitudinal study on a) Delaware, b) South Carolina, and c) Louisiana.

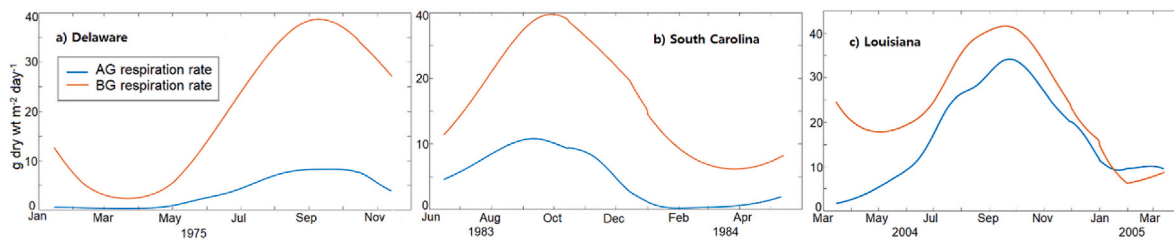


Fig. 5. Respiration rates of above- and below-ground biomass calculated by the PG model.

than plants grown at higher latitudes.

The model fitted well to the observed below-ground biomass in all three sites and both above- and below-ground biomass in South Carolina whereas it was not able to predict the pattern of the observed above-ground biomass in Delaware (Fig. 2). This deviation may occur while the model fits to the greater below-ground biomass and could fail to fit to the relative smaller above-ground biomass in the situation where the above- and below-ground biomass is different with a great degree like in Delaware.

The analysis of abiotic data shows that Louisiana provides the most favorable environment for plant growth. The highest average irradiance (14.77 mW cm^{-2}) and the highest mean annual temperature (20.4°C) was observed in Louisiana, compared to South Carolina (13.79 mW cm^{-2} , 19.1°C) and Delaware (14.63 mW cm^{-2} , 13.4°C). Differences between the maximum and the minimum annual temperatures were smallest in Louisiana compared to South Carolina and Delaware (Fig. 3). The longest growing seasons was also observed in Louisiana (Feb.–Nov.), followed by South Carolina (Feb.–Oct.) and Delaware (Mar.–Oct.). Kirwan et al. (2009) demonstrated that a significant latitudinal gradient in productivity is mainly determined by temperature and the length of growing season. Their simple linear regression showed an increase of $27 \text{ g m}^{-2} \text{ y}^{-1}$ in the end of season live *S. alterniflora* productivity with an increase of mean annual temperature by 1°C . Longstreth and Strain (1977) found that photosynthesis rates of *S. alterniflora* increase under high illumination. Thus, the high average irradiance and temperature with smaller annual temperature ranges could help plants photosynthesize, which result in more production in above-ground in Louisiana. This increased production may provide the capacity to translocate more carbon to below-ground tissues during the growing seasons.

The gross productions at all sites showed patterns similar to the regional temperature cycle, which support that the temperature is main driver in production (Fig. 3). The highest gross production rates ($40.19 \text{ g m}^{-2} \text{ d}^{-1}$) were observed in Louisiana, followed by South Carolina ($22.22 \text{ g m}^{-2} \text{ d}^{-1}$) and Delaware ($20.41 \text{ g m}^{-2} \text{ d}^{-1}$). The greater negative net production in Delaware was shown in the steady decrease in below-ground biomass during the study period. The below-ground biomass decreased from approximately 5000 g m^{-2} in January to 1100 g m^{-2} in July whereas the above-ground biomass fluctuated within a range between 660 and 1200 g m^{-2} throughout the year in Delaware. The relatively higher below-ground biomass compared to the above-ground biomass may cause more respiration than the production through photosynthesis, which in turn result in the negative net production. This result indicates that the net production rates cannot be explained simply by latitude but are site-specific although the gross production rates closely follow the environmental factor such as temperature and irradiance.

Interestingly, the carbon translocation from senescing above-ground tissues in the fall increases as the latitude increases, which support our second hypothesis. The highest amount and proportion (γ) (1703 g m^{-2} and 0.0024 , respectively) were observed at higher latitudes (Tables 5 and 6). This amount was more than three times that in Louisiana (458 g m^{-2}) during senescence. The pattern of mortality rates of both above- and below-ground peak during the late fall season, which in turn, may

generate more senescence in the above-ground biomass (Fig. 4). This may not only support the micro-organism food web in the soil but also enhance survival of *S. alterniflora*'s by storing carbon from senesced above-ground tissues in below-ground in preparation for the cold winter. This result suggests that photosynthates during growing season and the remobilization of assimilate from senescing shoots during fall seasons serve as the main two sources to grow the below-ground biomass in higher latitudes whereas the photosynthates generated in longer growing seasons are the main pathway to allocate carbon to the below-ground biomass in lower latitudes.

S. alterniflora grown in Delaware translocated assimilates from the below-ground tissues to above-ground (261 g m^{-2}) whereas the *S. alterniflora* in South Carolina and Louisiana allocated almost zero carbon during the dormancy period (Table 6). During fall and winter, the shoots in higher latitudes almost die and are often removed by ice and the tide before mid-winter (Gallagher, 1983), whereas the above-ground tissues survive through the winter in lower latitudes (Gallagher and Seliskar, 1976). The live above-ground biomass observed data in the study sites also showed a similar pattern. The live above-ground biomass was very consistent in Louisiana from November to the following March ranging 529 – 650 g m^{-2} whereas it dropped dramatically from 510 g m^{-2} in December to 84 g m^{-2} in January in South Carolina. The decreased winter above-ground biomass in higher latitudes may result in a higher amount of the assimilate translocation from below-to above-ground to sustain the above-ground tissues during winter seasons and support the shoot emergence in early spring. In South Carolina, the assimilate translocation (g m^{-2}) from below-to above-ground tissues during this period was observed to be almost zero. This suggests that in these regions, the photosynthates produced in the above-ground tissues are likely sufficient to meet the metabolic needs of the above-ground biomass, reducing the necessity for translocation from below-ground sources.

The mean below-ground respiration rates were similar, whereas the mean above-ground respiration rates were highest in Louisiana (Supplementary Table 2). These high rates may have been because of the higher temperature in Louisiana, since the respiration rates are positively correlated to the temperature in the model. The mean above-ground respiration rate in South Carolina ($4.79 \text{ g m}^{-2} \text{ d}^{-1}$) was similar with that in the tall form *S. alterniflora* on Sapelo Island ($3.60 \text{ g m}^{-2} \text{ d}^{-1}$) of the preliminary study whereas the mean below-ground respiration rate in South Carolina was about 3 folds that for Sapelo Island. This higher below-ground respiration rates could be due to the greater below-ground biomass ranging from 1600 to 3400 g m^{-2} in South Carolina compared to that on Sapelo Island ranging from 200 to 2000 g m^{-2} .

Overall, *S. alterniflora* at higher latitudes (Delaware) appears to store relatively more below-ground biomass than plants grown at lower latitudes (South Carolina and Louisiana), along with the higher root:shoot ratio. It appears that the maximum above-ground biomass is achieved earlier (Aug.) in the Delaware marshes than in the marshes of South Carolina and Louisiana (Oct.). Valiela et al. (1976) reported that the maximum aerial biomass was observed in early July in Massachusetts in 1971 and 1973. In the same years, Gallagher et al. (1980) discovered that the peak above-ground biomass occurred in August or September in

the Duplin estuary marsh in Georgia. The below-ground biomass increases after the formation of flowers (Crosby et al., 2015) and as senescing tissues start to increase (Elsey-Quirk et al., 2011). Thus, the rapid growth early in the short growing season in Delaware may enable *S. alterniflora* to complete their flowering cycles before the onset of winter as was observed in alpine plants (Mooney and Billings, 1960), which in turn, advances the timing of translocating biomass to below-ground.

It is hard to generalize the latitudinal pattern of translocation between above- and below-ground biomass from our study results due to the limited number of sites we studied and the short duration of observational data. However, the model analysis suggests that the different translocation pathways of *S. alterniflora* between above- and below-ground tissues need to be considered and that these differ according to the latitude. Furthermore, this study underscores the value of a mathematical model in enhancing the analysis and interpretation of field observations. It not only facilitates the derivation of physiological plant parameters but also aids in identifying discrepancies between model predictions and observed data. This dual capability is crucial for refining models and improving our understanding of plant processes. The model also helps us quantify the photosynthates or assimilate translocation at each phenological cycle and understand the main sources of the below-ground biomass allocation by latitudes which are hard to grasp in field experiments. Future research could further refine the model by incorporating the mechanisms of phenology, with particular attention to soil temperature, a critical factor in green-up phenology (Zhang et al., 2004).

5. Summary

The model results show good match with the below-ground field data in all latitudes and both above- and below-ground biomass for *S. alterniflora* in South Carolina. The model analysis showed that *S. alterniflora* in higher latitudes experiences a modest amount of assimilate translocation from below-to above-ground tissues during the dormancy period, while this translocation is nearly negligible in lower latitudes. The main sources of translocating carbon to below-ground tissues in *S. alterniflora* varied by latitude. *S. alterniflora* in a lower latitude with a warmer climate allocates mainly from the photosynthates produced in the above-ground tissues to the below-ground tissues during the longer growing seasons, whereas *S. alterniflora* in higher latitudes utilize the translocation both from photosynthates during the growing season and assimilate from the senescing plant tissues during the fall. The below-ground respiration rates of plants are generally consistent across latitudes, while the above-ground rates are highest in lower latitudes, likely due to warmer temperatures in these regions. This research underscores the necessity of accounting for varying translocation dynamics across latitudes to precisely evaluate the growth and translocation pathways in *S. alterniflora* throughout its phenological cycles. Furthermore, the study enhances our understanding of the mechanisms through which carbon, assimilated by salt marsh grass, is sequestered and redistributed within its blue carbon ecosystem.

CRediT authorship contribution statement

Yeajin Jung: Writing – review & editing, Writing – original draft, Visualization, Validation, Investigation.

Declaration of competing interest

The authors declare that they have no known competing financial interests or personal relationships that could have appeared to influence the work reported in this paper.

Data availability

Data will be made available on request.

Acknowledgement

This work was funded by a National Science Foundation grant (OCE-1237140) and with support from the University of Georgia Graduate School. I would like to thank A. Burd, M. Alber, S. Pennings, J. Morris, and L. Donovan for helpful discussions and advise, C. Roman for providing field data.

Appendix A. Supplementary data

Supplementary data to this article can be found online at <https://doi.org/10.1016/j.ecss.2023.108587>.

References

Asaeda, T., Hai, D.N., Manatunge, J., Williams, D., Roberts, J., 2005. Latitudinal characteristics of below-and above-ground biomass of *Typha*: a modelling approach. *Annal. Bot.* 96 (2), 299–312.

Asaeda, T., Karunarathne, S., 2000. Dynamic modeling of the growth of *Phragmites australis*: model description. *Aquat. Bot.* 67 (4), 301–318.

Bertin, R.J., 2008. Plant phenology and distribution in relation to recent climate change. *J. Torrey Bot. Soc.* 135 (1), 126–146. <https://doi.org/10.3159/07-Rp-035r.1>.

Bertness, M.D., Ewanchuk, P.J., 2002. Latitudinal and climate-driven variation in the strength and nature of biological interactions in New England salt marshes. *Oecologia* 132 (3), 392–401.

Callaway, J.C., 1990. *The Introduction of *Spartina alterniflora* in south San Francisco Bay* (Master Thesis). San Francisco State University, San Francisco, CA.

Callaway, J.C., Josselyn, M.N., 1992. The introduction and spread of smooth cordgrass (*Spartina alterniflora*) in South San Francisco Bay. *Estuaries* 15 (2), 218–226. <https://doi.org/10.2307/1352695>.

Chuine, I., Beaubien, E.G., 2001. Phenology is a major determinant of tree species range. *Ecol. Lett.* 4 (5), 500–510.

Chuine, I., Cambon, G., Comtois, P., 2000. Scaling phenology from the local to the regional level: advances from species-specific phenological models. *Global Change Biol.* 6 (8), 943–952.

Cleland, E.E., Chuine, I., Menzel, A., Mooney, H.A., Schwartz, M.D., 2007. Shifting plant phenology in response to global change. *Trends Ecol. Evol.* 22 (7), 357–365.

Cranford, P.J., Gordon, D.C., Jarvis, C.M., 1989. Measurement of cordgrass, *Spartina alterniflora*, production in a macrotidal estuary, Bay of Fundy. *Estuaries* 12 (1), 27–34.

Crosby, S.C., Ivens-Duran, M., Bertness, M.D., Davey, E., Deegan, L.A., Leslie, H.M., 2015. Flowering and biomass allocation in U.S. Atlantic coast *Spartina alterniflora*. *Am. J. Bot.* 102 (5), 669–676. <https://doi.org/10.3732/ajb.1400534>.

Dame, R.F., Kenny, P.D., 1986. Variability of *Spartina alterniflora* primary production in the euhaline North Inlet estuary. *Mar. Ecol. Prog. Ser.* 32 (1), 71–80.

Darby, F.A., Turner, R.E., 2008. Below-and aboveground biomass of *Spartina alterniflora*: response to nutrient addition in a Louisiana salt marsh. *Estuar. Coast* 31 (2), 326–334.

Davis, J.L., Currin, C.A., O'Brien, C., Raffenburg, C., Davis, A., 2015. Living shorelines: coastal resilience with a blue carbon benefit. *PLoS One* 10 (11), e0142595.

Ehrlén, J., Morris, W.F., 2015. Predicting changes in the distribution and abundance of species under environmental change. *Ecol. Lett.* 18 (3), 303–314. <https://doi.org/10.1111/ele.12410>.

Eleuterius, L.N., Caldwell, J.D., 1984. Flowering phenology of tidal marsh plants in Mississippi. *Castanea* 49 (4), 172–179.

Elsey-Quirk, T., Seliskar, D.M., Gallagher, J.L., 2011. Differential population response of allocation, phenology, and tissue chemistry in *Spartina alterniflora*. *Plant Ecology*, 212 (11), 1873–1885.

Euskirchen, E.S., Carman, T.B., McGuire, A.D., 2014. Changes in the structure and function of northern Alaskan ecosystems when considering variable leaf-out times across groupings of species in a dynamic vegetation model. *Global Change Biol.* 20 (3), 963–978.

Fenner, M., 1998. The phenology of growth and reproduction in plants. *Perspect. Plant Ecol. Evol. Systemat.* 1 (1), 78–91.

Gallagher, J.L., 1983. Seasonal patterns in recoverable underground reserves in *Spartina alterniflora* Loisel. *Am. J. Bot.* 70 (2), 212–215.

Gallagher, J.L., Seliskar, D.M., 1976. The Metabolism of Senescent *Spartina alterniflora*. *Annual Meeting Botany Society of America, New Orleans Abstract*, p. 34.

Gallagher, J.L., Reimold, R.J., Linthurst, R.A., Pfeiffer, W.J., 1980. Aerial production, mortality, and mineral accumulation-export dynamics in *Spartina alterniflora* and *Juncus roemerianus* plant stands in a Georgia salt marsh. *Ecology* 61 (2), 303–312. <https://doi.org/10.2307/1935189>.

Ge, Z.M., Zhang, L.Q., Yuan, L., Zhang, C., 2014. Effects of salinity on temperature-dependent photosynthetic parameters of a native C3 and a non-native C4 marsh grass in the Yangtze Estuary, China. *Photosynthetica* 52 (4), 484–492.

Gross, M.F., Hardisky, M.A., Wolf, P.L., Klemas, V., 1991. Relationship between aboveground and belowground biomass of *Spartina alterniflora* (smooth cordgrass). *Estuaries* 14 (2), 180–191.

Heimann, M., Esser, G., Haxeltine, A., Kaduk, J., Kicklighter, D.W., Knorr, W., et al., 1998. Evaluation of terrestrial carbon cycle models through simulations of the seasonal cycle of atmospheric CO₂: first results of a model intercomparison study. *Global Biogeochem. Cycles* 12 (1), 1–24.

Howes, B.L., Howarth, R.W., Teal, J.M., Valiela, I., 1981. Oxidation-reduction potentials in a salt marsh: spatial patterns and interactions with primary production 1. *Limnol. Oceanogr.* 26 (2), 350–360. <https://doi.org/10.4319/lo.1981.26.2.0350>.

Iqbal, M., 1984. An introduction to solar radiation. Elsevier. <https://doi.org/10.1016/B978-0-12-373750-2.X5001-0>.

Jung, Y., Burd, A., 2017. Seasonal changes in above- and below-ground non-structural carbohydrates (NSC) in *Spartina alterniflora* in a marsh in Georgia, USA. *Aquat. Bot.* 140, 13–22. <https://doi.org/10.1016/j.aquabot.2017.04.003>.

Jung, Y., Burd, A., 2024. Carbon allocation dynamics of *Spartina alterniflora* in Georgia saltmarsh, USA in preparation.

Kirk, J.T.O., 1994. Light and Photosynthesis in Aquatic Ecosystems. Cambridge University Press.

Kirwan, M.L., Guntenspergen, G.R., Morris, J.T., 2009. Latitudinal trends in *Spartina alterniflora* productivity and the response of coastal marshes to global change. *Global Change Biol.* 15 (8), 1982–1989.

Kramer, K., 1994. Selecting a model to predict the onset of growth of *Fagus sylvatica*. *J. Appl. Ecol.* 31 (1), 172–181. <https://doi.org/10.2307/2404609>.

Livingstone, D.C., Patriquin, D.G., 1981. Belowground growth of *Spartina alterniflora* Loisel.: habit, functional biomass and non-structural carbohydrates. *Estuar. Coast Shelf Sci.* 12 (5), 579–587.

Longstreth, D.J., Strain, B.R., 1977. Effects of salinity and illumination on photosynthesis and water balance of *Spartina alterniflora* Loisel. *Oecologia* 31 (2), 191–199.

Lytle, R.W., Hull, R.J., 1980. Photoassimilate distribution in *Spartina alterniflora* Loisel. II. autumn and winter storage and spring regrowth 1. *Agron. J.* 72 (6), 938–942.

Mooney, H.A., Billings, W.D., 1960. The annual carbohydrate cycle of alpine plants as related to growth. *Am. J. Bot.* 47 (7), 594–598. <https://doi.org/10.2307/2439439>.

Morris, J.T., 1982. A model of growth responses by *Spartina alterniflora* to nitrogen limitation. *J. Ecol.* 70 (1), 25–42. <https://doi.org/10.2307/2259862>.

Morris, J.T., Haskin, B., 1990. A 5-yr record of aerial primary production and stand characteristics of *Spartina alterniflora*. *Ecology* 71 (6), 2209–2217.

Morris, J.T., Houghton, R.A., Botkin, D.B., 1984. Theoretical limits of belowground production by *Spartina alterniflora*: an analysis through modelling. *Ecol. Model.* 26 (3), 155–175. [https://doi.org/10.1016/0304-3800\(84\)90068-1](https://doi.org/10.1016/0304-3800(84)90068-1).

Ning, Z., Chen, C., Xie, T., Zhu, Z., Wang, Q., Cui, B., Bai, J., 2021. Can the native faunal communities be restored from removal of invasive plants in coastal ecosystems? A global meta-analysis. *Global Change Biol.* 27 (19), 4644–4656.

O'Donnell, J., Schalles, J., 2016. Examination of abiotic drivers and their influence on *Spartina alterniflora* biomass over a twenty-eight year period using landsat 5 TM satellite imagery of the central Georgia coast. *Rem. Sens.* 8 (6), 1–22.

Qi, X., Chmura, G.L., 2023. Invasive *Spartina alterniflora* marshes in China: a blue carbon sink at the expense of other ecosystem services. *Front. Ecol. Environ.* 21 (4), 182–190.

Roman, C.T., Daiber, F.C., 1984. Aboveground and belowground primary production dynamics of two Delaware bay tidal marshes. *Bull. Torrey Bot. Club* 111 (1), 34–41. <https://doi.org/10.2307/2996208>.

Smalley, A.E., 1958. *The Role of Two Invertebrate Populations, Littorina irrorata and Orchestium fiducinum in the Energy Flow of a Salt Marsh Eco- System* (Doctoral Dissertation). University of Georgia, Athens, GA.

Turner, R.E., Gosselink, J.G., 1975. *A note on standing crops of Spartina alterniflora in Texas and Florida*. Louisiana State University.

Unger, V., Elsey-Quirk, T., Sommerfield, C., Velinsky, D., 2016. Stability of organic carbon accumulating in *Spartina alterniflora*-dominated salt marshes of the Mid-Atlantic US. *Estuar. Coast Shelf Sci.* 182, 179–189.

Valiela, I., Teal, J.M., Persson, N.Y., 1976. Production and dynamics of experimentally enriched salt marsh vegetation: belowground biomass 1. *Limnol. Oceanogr.* 21 (2), 245–252. <https://doi.org/10.4319/lo.1976.21.2.0245>.

Van Wijk, M.T., Williams, M., 2003. Interannual variability of plant phenology in tussock tundra: modelling interactions of plant productivity, plant phenology, snowmelt and soil thaw. *Global Change Biol.* 9 (5), 743–758.

Zhang, X., Friedl, M.A., Schaaf, C.B., Strahler, A.H., 2004. Climate controls on vegetation phenological patterns in northern mid-and high latitudes inferred from MODIS data. *Global Change Biol.* 10 (7), 1133–1145.

Zheng, S., Shao, D., Asaeda, T., Sun, T., Luo, S., Cheng, M., 2016. Modeling the growth dynamics of *Spartina alterniflora* and the effects of its control measures. *Ecol. Eng.* 97, 144–156. <https://doi.org/10.1016/j.ecoleng.2016.09.006>.